Trapping energy of a spherical particle on a curved liquid interface

Joseph Léandri, Alois Würger

Trapping energy of a spherical particle on a curved liquid interface

Joseph Léandri and Alois Würger
LOMA, Université de Bordeaux & CNRS, 351 cours de la Libération, 33405 Talence, France

We derive the trapping energy of a colloidal particle at a liquid interface with contact angle θ and principal curvatures c_1 and c_2. The boundary conditions at the particle surface are significantly simplified by introducing the shift ε of its vertical position. We discuss the undulating contact line and the curvature-induced lateral forces for a single particle and a pair of nearby particles. The single-particle trapping energy is found to decrease with the square of both the total curvature $c_1 + c_2$ and the anisotropy $c_1 - c_2$. In the case of non-uniform curvatures, the resulting lateral force pushes particles toward more strongly curved regions.

PACS numbers:

I. INTRODUCTION

Colloidal particles trapped at a liquid phase boundary are subject to capillary forces which induce pattern formation and directed motion [1–3], and contribute to stabilize Pickering emulsions and particle aggregates [4, 5]. Such microstructures affect the mechanical and flow behavior of liquid and gel phases [6], which in turn are relevant for material properties and biotechnological applications [7]. In many instances, the particles are trapped at curved liquid interfaces; rather surprisingly, even for spherical particles the influence of curvature on capillary forces is not fully understood at present.

At a flat interface, capillary phenomena arise from normal forces induced by the particle's weight or charge, or from geometrical constraints due to its shape [8, 9]. As a simple example, an oat grain floating on a cup of milk is surrounded by a meniscus that results from the its weight and buoyancy; the superposition of the dimples of nearby grains reduces the surface energy and thus causes aggregation. Charged beads exert electric stress on the interface. The meniscus overlap of nearby particles causes a repulsive electrocapillary potential [10, 11], whereas beyond the superposition approximation, a significantly larger attractive term is found [12–14]. In the absence of gravity and electric forces, capillary phenomena still occur for non-spherical particles: A capillary quadrupole may arise from surface irregularities [15, 16], pinning of the contact line [17], and for ellipsoids [18–21], and favors the formation of clusters with strong orientational order.

A more complex situation occurs for interfaces with principal curvatures c_1 and c_2. The superposition of the weight-induced meniscus and the intrinsic curvature results in a coupling energy that is linear in the total curvature $H = c_1 + c_2$. Its spatial variation gives rise to a lateral force that drags a colloidal sphere along the curvature gradient [22, 23]. Non-spherical particles interact through their capillary quadrupole with the curvature difference $\delta c = c_1 - c_2$, and thus experience both a torque and lateral force [24]. The latter is well known from the locomotion of meniscus-climbing insects and larvae, which bend their body according to the local curvature

FIG. 1: Three-phase boundary of a spherical particle at a liquid interface with curvatures $c_2 = -\frac{1}{2}c_1$. The contact line is not a circle but undulates in space.

such that the capillary energy overcomes gravity [25, 26]; through a similar effect, ellipsoidal particles prevent ring formation of drying coffee stains [27, 28]. A recent experiment on micro-rods trapped at a water-oil meniscus illustrates both rotational and translational motion driven by curvature [3].

In this paper, we evaluate the geometrical part of the trapping energy of a spherical particle on a curved interface; thus we consider only terms that arise from the interface profile but are independent of body forces such as weight and buoyancy. Previous papers considered limiting cases such as a minimal surface ($H = 0$) [29], a spherical droplet ($\delta c = 0$) [30, 31], or a cylindrical interface ($H = \delta c$) [32]; yet a comprehensive picture is missing so far. Here we treat the general case where both H and δc are finite, and obtain the trapping energy in a controlled approximation to quadratic order in the curvature parameters. We resort to the usual assumptions of constant contact angle θ, curvature radius much larger than the particle size, and small meniscus gradient.

As an original feature of the formal apparatus, we introduce the curvature-induced shift ε of the vertical particle position as an adjustable parameter, in addition to the amplitude ξ_2 of the quadrupolar interface deformation. As a main advantage, the boundary conditions at the contact line separate in two independent equations

for ε and ξ_2, which are readily solved and provide a simple physical picture for the effects of the two curvature parameters.

The paper is organized as follows. Section 2 gives a detailed derivation of the energy functional and the deformation field $\xi(\mathbf{r})$. From the usual variational procedure we find in section 3 the energy as a function of the curvature parameters and the unkowns ε and ξ_2; then the energy is minimized with respect to the unknowns ε and ξ_2. In section 4 we show that the solution satisfies Young's law at the three-phase boundary. In Section 5 we compare the trapping energy with previous work, and discuss the contact line and curvature-induced forces. Section 6 contains a brief summary.

II. TRAPPING ENERGY

Here we derive the expression for the trapping energy and then evaluate it explicitly to quadratic order in the curvatures. It consists of the surface energies of all phase boundaries and the work done by the Laplace pressure both on the liquid interface and on the area occupied by the particle.

First consider a particle dispersed in the liquid phase with the smaller surface tension $\gamma_m = \min(\gamma_1, \gamma_2)$. The total energy

$$\gamma S_0 + W_0 + \gamma_m 4\pi a^2$$

accounts for the interface area S_0, the work W_0, and for the particle surface $4\pi a^2$, as illustrated in Fig. 3a.

A particle approaching the interface gets trapped if the surface tensions satisfy the inequality $|\gamma_1 - \gamma_2| < \gamma$. The situation shown in Fig. 3 corresponds to $\gamma_m = \gamma_2$. The total energy

$$\gamma S + W + \gamma_1 S_1 + \gamma_2 S_2$$

consists of a term γS proportional to the area of the liquid interface, the work W, and the particle segments in contact with the two phases, $\gamma_1 S_1 + \gamma_2 S_2$.

The trapping potential is given by the energy difference of these two situations,

$$E = \gamma(S - S_0) + W - W_0 + \gamma_1 S_1 + \gamma_2 S_2 - \gamma_m 4\pi a^2. \quad (1)$$

As illustrated in Fig. 3b, S is smaller than the unperturbed area S_0. Since Young's law needs to be satisfied everywhere along the three-phase contact line, S may show a significantly more complex profile than S_0.

In this section we evaluate the trapping energy to second order in the curvature. There are two issues requiring particular care. First, both the particle surface and the liquid interface contribute linear terms which, however, cancel each other. Second, at quadratic order, there are various contributions from the liquid interface, the area occupied by the particle, and the work done by the Laplace pressure; these terms carry comparable prefactors but opposite sign. The main result is given in Eq. (18) below.

A. Flat interface $H = 0 = \delta c$

We briefly recall the well-known results for zero curvature $w_0 = 0$, where both S_0 and S are flat [1]. Imposing local mechanical equilibrium relates the surface tension parameters to the contact angle θ at the three-phase line in terms of Young's law

$$\gamma_1 - \gamma_2 = \gamma \cos\theta. \quad (2)$$

Then the area of the liquid interface is reduced by

$$S - S_0 = -\pi r_0^2,$$

and the segments of the particle surface read

$$S_1 = 2\pi a^2 - 2\pi a z_0, \qquad S_2 = 2\pi a^2 + 2\pi a z_0.$$

Here and in the following we use the vertical and radial coordinates of the contact line,

$$z_0 = a\cos\theta, \qquad r_0 = a\sin\theta,$$

as illustrated in the left panel of Fig. 2. With Young's law one finds for a flat interface [1],

$$E_F = -\pi a^2 \gamma (1 - |\cos\theta|)^2. \quad (3)$$

The trapping energy vanishes for contact angles $\theta = 0$ and $\theta = \pi$. For $|\gamma_1 - \gamma_2| > \gamma$ Young's law has no solution, meaning that there is no stable trapped state. In the remainder of this section we consider corrections to E_F that arise at a curved interface.

B. Curved interface without particles

Now we consider the case of finite curvature. In Monge representation, $w_0(u, v)$ gives the interface height with respect to a tangent plane with coordinates u and v. The energy consists of two terms,

$$\gamma S_0 + W_0 = \gamma \int dA \left(1 + \frac{1}{2}\left(\nabla w_0\right)^2\right) - \int dA w_0 P, \quad (4)$$

the first of which describes the interface energy [29], and the second one the work done by the pressure difference P between the two sides of the interface. Here we have already used the small-gradient approximation $|\nabla w_0| \ll 1$; for its derivation see [29]. Its range of validity depends on the actual shape of the interface; for experimentally relevant situations one finds that this approximation is justified for distances wihtin the curvature radius. Since both the profile w_0 and the pressure P turn out to be linear in H and δc, Eq. (4) is exact to second order in the curvature parameters.

The minumum-energy profile is determined by linearizing in terms of a small fluctuation δw_0; integrating by parts one finds the corresponding variation of energy

$$\delta E = -\int dA\ \delta w_0 \left(\gamma \nabla^2 w_0 + P\right).$$

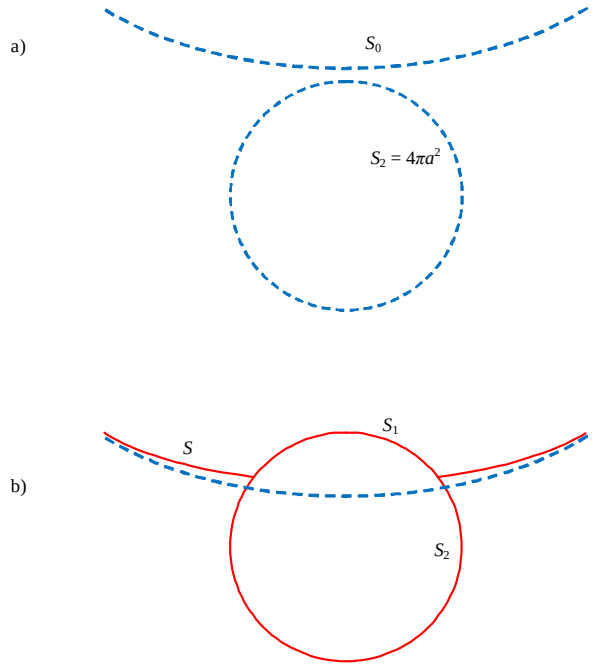

FIG. 2: Surface and interface areas contributing to the trapping energy in Eq. (1). The upper liquid is labelled "1" and the lower "2". a) The particle is in the phase of lower surface energy (here $\gamma_2 < \gamma_1$); the liquid interface of area S_0 is described by (6). b) Trapped state. The presence of the particle reduces the area of the liquid phase boundary to the value S and deforms its profile. The surface areas S_1 and S_2 are in contact with the two liquid phases. Note that the figure shows one vertical section of the interface; both S_0 and S undulate when rotating about the vertical axis.

Searching for a solution that is stable with respect to any small deformation δw_0, we require $\delta E = 0$ and thus find the Young-Laplace equation

$$\boldsymbol{\nabla}^2 w_0 + P/\gamma = 0, \tag{5}$$

which relates the profile to the pressure difference P and the tension γ.

If the Laplace pressure varies sufficiently slowly along the interface, one has $w_0 = \frac{1}{2}\left(c_1 u^2 + c_2 v^2\right)$, with the coordinates u and v along the local principal curvature axes. For later convenience we transform to polar coordinates; inserting $u = r\cos\varphi$ and $v = r\sin\varphi$, resulting in

$$w_0\left(r,\varphi\right) = \frac{r^2}{4}\left(H + \delta c\ \cos(2\varphi)\right). \tag{6}$$

The axes are chosen such that both H and δc are positive. Note that the "mean curvature" is often defined as $H' = \frac{1}{2}(c_1 + c_2)$ and thus differs from our H by a factor $\frac{1}{2}$.

The Young-Laplace equation relates the mean curvature to the pressure according to

$$P = -\gamma H, \tag{7}$$

whereas an asymmetry δc is usually imposed by appropriate boundary conditions. Eq. (7) takes a particularly simple form on a sphere of radius R, where the curvature $H = 2/R$ is related to the excess pressure $2\gamma/R$ inside the droplet.

Many experiments proble spatial variations of the curvature parameters H and δc, which occur on a scale that is at least of the order the curvature radius

$$R = 2/\sqrt{H^2 + \delta c^2}.$$

Thus the quadratic form (6) provides a good approximation for the interface profile at distances within the curvature radius.

C. Curved interface with a trapped particle

Now we add a colloidal particle to the interface (6). Like previous papers, the present work relies on the separation of length scales, assuming that the characteristic length of the deformation induced by a colloidal particle of size a, is much larger than that of the unperturbed interface, R. All approximate formulae of the present paper can be cast in the form of a truncated series in powers of a/R, and the trapping energy derived below is exact to quadratic order.

Because of the undulating contact line, Young's law cannot be satisfied along the intersection of $w_0(r,\varphi)$ and the spherical bead, but requires a modified interface profile

$$w = w_0 + \xi, \tag{8}$$

which is the sum of the unperturbed w_0 and the deformation field ξ. The latter has to be chosen such that the total energy is minimum.

The deformation field ξ affects the trapping energy in three respects: First, it modifies the work done by the Laplace pressure, second, it results in a more complex profile of the liquid interface S and, third, it modifies the contact line, that is, the common boundary of S, S_1, and S_2.

We start with the change in work due to the presence of a trapped particle. It turns out convenient to separate the parameter space in domains $\mathcal{I}$ and $\mathcal{P}$, where $\mathcal{I}$ is the projection of the liquid interface on the tangential plane and $\mathcal{P}$ the part occupied by the particle. Then the work function reads

$$W - W_0 = \int_{\mathcal{I}} dA(w_0 - w)P + \int_{\mathcal{P}} dA(w_0 + \varepsilon)P. \tag{9}$$

The first integral may be viewed as the change of potential energy of the interface in the pressure field. The

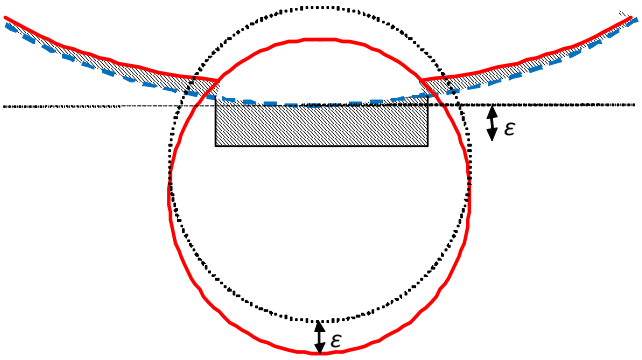

FIG. 3: The hatched area gives a schematic view of the volume of the work done by the Laplace pressure in Eq. (9). The volume corresponding to the interface domain $\mathcal{I}$ reads $\int dA(w_0 - w)$, and that over $\mathcal{P}$ reads $\int dA(w_0 + \varepsilon)$, where ε is the vertical change of the particle position. The reference state on a flat interface is shown as dotted lines. Solid and dashed lines as in Fig. 2b.

second one is proportional to the vertical position of the particle with respect to the unperturbed interface. In our notation, $\varepsilon > 0$ corresponds to a downward motion of the particle. In Fig. 3he integration volume is shown as hatched area.

Now we turn to the modification of the liquid-interface area $S - S_0$. Though the formally exact expressions can be given in terms of $\boldsymbol{\nabla} w$ and $\boldsymbol{\nabla} w_0$, [29], we immediately use the the small-gradient approximation and thus find

$$\begin{aligned} S - S_0 &= \frac{1}{2}\int_{\mathcal{I}} dA \left((\boldsymbol{\nabla} w)^2 - (\boldsymbol{\nabla} w_0)^2 \right) \\ &\quad - \int_{\mathcal{P}} dA \left(1 + \frac{1}{2} (\boldsymbol{\nabla} w_0)^2 \right). \end{aligned} \tag{10}$$

The first integral accounts for the change of area of the deformed interface, and the second one for the area occupied by the particle; the corresponding parameter domains are $\mathcal{I}$ and $\mathcal{P}$.

Finally, we evaluate the change of the surface energy of the particle. The segments in contact with the two liquid phases are given by the vertical coordinate $\widetilde{z}(\varphi)$ of the contact line with respect to the particle center,

$$S_{1/2} = 2\pi a^2 \mp 2\pi a \int_0^{2\pi} d\varphi \widetilde{z}. \tag{11}$$

Their sum obviously gives $4\pi a^2$.

III. ENERGY MINIMIZATION

The trapping energy (1) is a functional of the deformation field $\xi(\mathbf{r})$ and moreover depends on the vertical position parameter ε. In a first step we minimize $E[\xi]$ with respect to the shape function ξ, and thus obtain the trapping energy as a function of the deformation amplitude and the vertical position. In a second step we minimize with respect to the latter parameters, and thus obtain the energy in terms of the curvature parameters.

A. Deformation field

Linearizing both $S - S_0$ and $W - W_0$ in terms of a fluctuation $\delta\xi$ and integrating by parts, we find [29]

$$\delta E = -\int_{\mathcal{I}} dA\ \delta\xi \left(\gamma \boldsymbol{\nabla}^2 \xi + \gamma \boldsymbol{\nabla}^2 w_0 + P \right).$$

The last two terms in parentheses cancel in view of Eq. (5). The requirement that the energy be extremum, $\delta E = 0$ for any $\delta\xi$, directly leads to

$$\boldsymbol{\nabla}^2 \xi = 0. \tag{12}$$

In other words, the deformation satisfies the equation of a minimal surface.

Integrating by parts and using (12), we find for the first term in (10)

$$-\int_{\mathcal{I}} dA \xi \boldsymbol{\nabla}^2 w_0 + \frac{1}{2}\oint_{\partial\mathcal{I}} d\mathbf{s}\cdot \left(\boldsymbol{\nabla}\xi + 2\boldsymbol{\nabla} w_0 \right) \xi.$$

From the Young-Laplace equation it is clear that the integral over $\mathcal{I}$ cancels the first term of the work (9). Inserting the remainder in (1) we obtain

$$\begin{aligned} E &= \frac{1}{2}\oint_{\partial\mathcal{I}} d\mathbf{s}\cdot \left(\boldsymbol{\nabla}\xi + 2\boldsymbol{\nabla} w_0 \right) \xi \\ &\quad - \int_{\mathcal{P}} dA \left(\gamma + \frac{\gamma}{2} (\boldsymbol{\nabla} w_0)^2 - (w_0 + \varepsilon) P \right) \\ &\quad + \gamma_1 S_1 + \gamma_2 S_2 - \gamma_m 4\pi a^2. \end{aligned} \tag{13}$$

B. Truncation at second order

Since the interface areas S_0 and S are correct to second order in the curvature, the different terms in the above energy are significant only to quadratic order in the curvature and deformation parameters.

The general solution of (12) reads $\xi_0 \ln r + \sum_k \xi_k (r_0/r)^k \cos(k\varphi)$. The logarithmic term vanishes in the absence of an external force such as gravity; contributions with k odd are absent for a spherical particle. Because of the twofold symmetry of the source field (6), the quadrupolar term $k = 2$ is the only contribution that is linear in the curvature, the remaining coefficients are of least quadratic order. Thus we write

$$\xi(r, \varphi) = \xi_2 (r_0/r)^2 \cos(2\varphi) \tag{14}$$

and discard quadratic and higher-order terms in ξ. For notational convenience we rewrite the unperturbed interface in the form

$$w_0(r, \varphi) = \frac{r^2}{r_0^2} \left(\omega_0 + \omega_2 \cos(2\varphi) \right),$$

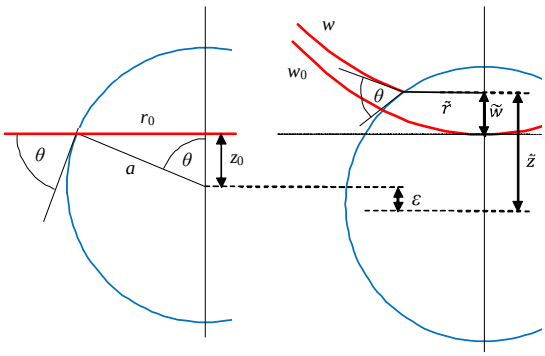

FIG. 4: Side view on a sphere trapped at a liquid phase boundary. The left panel shows a flat interface, where $r_0 = a\sin\theta$ and $z_0 = a\cos\theta$ are the radial and vertical coordinates of the contact line with respect to the particle center. The right panel illustrates the case of finite curvature. In a vertical section of given azimuth, we show both the unperturbed interface w_0 and the deformed profile w. Two phenomena concur in order to satisfy Young's law: The interface profile changes by $\xi = w - w_0$, and the particle adjusts its vertical position by ε. Besides its radial coordinate $\tilde{r}$, we indicate the vertical position of the contact line with respect to the tangent plane, $\tilde{w}$, and with respect to the particle center, $\tilde{z} = z_0 + \tilde{w} + \varepsilon$. In the case of finite curvature anisotropy δc, the contact line is not a circle but undulates along the particle surface, as illustrated by the top view in Fig. 4.

with the parameters

$$\omega_0 = \frac{1}{4}Hr_0^2, \qquad \omega_2 = \frac{1}{4}\delta c r_0^2. \tag{15}$$

C. The contact line

For further use we specify the radial and vertical coordinates $\widetilde{r}$ and $\widetilde{z}$ of the undulating contact line. The curvature-induced change of the vertical position with respect to that on a flat interface comprises two terms,

$$\widetilde{z} = z_0 + \widetilde{w} + \varepsilon, \tag{16}$$

where $\widetilde{w} = w_0(\widetilde{r}) + \xi(\widetilde{r})$ accounts for the vertical displacement of the contact line on the particles surface, and ε for the change in the particle position with respect to the tangential plane, as illustrated in the right panel of Fig. 2. Any point at the surface of the sphere satisfies the condition $\widetilde{r}^2 + \widetilde{z}^2 = a^2$, which can be rewritten as

$$\widetilde{r}^2 = r_0^2 - 2z_0\,(\widetilde{w} + \varepsilon) - (\widetilde{w} + \varepsilon)^2. \tag{17}$$

D. Evaluation of E

In the following we evaluate the trapping energy (13) to second order in the curvature parameters ω_0 and ω_2, the deformation amplitude ξ_2, and the vertical shift ε. Since the integrand of the contour along $\partial\mathcal{I}$ is already of second order, we take $d\mathbf{s} = -\mathbf{e}_r r_0 d\varphi$, reduce the gradients to the radial components $\partial_r\widetilde{\xi} + 2\partial_r\widetilde{w}_0$, and replace the coordinate $\widetilde{r}$ of the contact line with r_0,

$$\frac{1}{2}\oint_{\partial\mathcal{I}} d\mathbf{s}\cdot\left(\boldsymbol{\nabla}\xi + 2\boldsymbol{\nabla}w_0\right)\xi = \pi\gamma\xi_2^2 - 2\pi\gamma\xi_2\omega_2.$$

The first term of the area integral is readily evaluated in terms of $dA = \frac{1}{2}\widetilde{r}^2 d\varphi$; expanding $\widetilde{r}^2$ to second order in the small parameters we find

$$\int_{\mathcal{P}} dA = \pi r_0^2 - 2\pi z_0(\omega_0 + \varepsilon) - \pi(\omega_0 + \varepsilon)^2 - \frac{\pi}{2}(\omega_2 + \xi_2)^2.$$

In the following term the integrand $(\boldsymbol{\nabla}w_0)^2$ is already of second order in the curvature; thus we may replace the radius of the contact line with r_0 and obtain

$$\frac{1}{2}\int_{\mathcal{P}} dA(\boldsymbol{\nabla}w_0)^2 = \pi\gamma\left(\omega_0^2 + \omega_2^2\right).$$

Noting $P = -\gamma H = -4\gamma\omega_0/r_0^2$, the work done on the area occupied by the particle gives

$$\int_{\mathcal{P}} dA(w_0 + \varepsilon)P = -2\pi\gamma\omega_0\left(\omega_0 + 2\varepsilon\right).$$

Finally, we evaluate the change of the surface energy of the particle,

$$S_{1/2} = 2\pi a^2 \mp 2\pi a(z_0 + \omega_0 + \varepsilon).$$

Inserting these expressions in (1), separating the terms on a flat interface, and replacing the surface tensions γ_1 and γ_2 through Young's law (2), we find

$$\begin{aligned} E - E_F \;=\; & \frac{3}{2}\pi\gamma\xi_2^2 - \pi\gamma\xi_2\omega_2 - \frac{\pi}{2}\gamma\omega_2^2 \\ & + \pi\gamma\varepsilon^2 - 2\pi\gamma\omega_0\varepsilon - 2\pi\gamma\omega_0^2. \end{aligned} \tag{18}$$

Besides the curvature parameters ω_0 and ω_2, this energy depends on two unknown parameters, the deformation amplitude ξ_2 and the vertical shift ε of the particle position with respect to its value on a flat interface.

E. Minimum energy

The energy minimum is obtained from the zero of the derivatives with respect to the adjustable parameters ξ_2 and ε,

$$\frac{dE}{d\varepsilon} = 0 = \frac{dE}{d\xi_2}. \tag{19}$$

From (18) one readily finds the corresponding values

$$\varepsilon = \omega_0, \qquad \xi_2 = \omega_2/3. \tag{20}$$

In physical terms, the mean curvature H results in a shift ε of the particle toward the convex side of the interface. (In Fig. 3 this means in downward direction.) On the other hand, the non-uniform curvature δc gives rise to the quadrupolar amplitude ξ_2, which in turn enhances the angular modulation of the interface.

Inserting the above values for ε and ξ_2 in the trapping energy, we find

$$E = E_F - 3\pi\gamma\omega_0^2 - \frac{2}{3}\pi\gamma\omega_2^2. \tag{21}$$

IV. YOUNG'S LAW AT THE CONTACT LINE

The curvature-dependent part of E has been calculated by minimizing the total trapping energy with respect to the unknowns ε and ξ_2, without resorting to Young's law for the contact angle at the three-phase boundary. Since Young's law is nothing else but the local condition for a minimum-energy state, it expresses the same physical constraint as Eq. (19) and thus provides an independent means of checking the above results.

This is achieved by imposing the contact angle θ along the three-phase boundary. We start from the form [29]

$$\cos\theta = \mathbf{n}_I \cdot \mathbf{n}_P, \tag{22}$$

where $\mathbf{n}_I$ is the normal vector on the interface and $\mathbf{n}_P$ the normal on the particle surface. The former is best given in Monge gauge with respect to the vertical axis, and the latter takes a simple form because of the spherical geometry,

$$\mathbf{n}_I = \frac{\mathbf{e}_z - \boldsymbol{\nabla}\widetilde{w}}{\sqrt{1+(\boldsymbol{\nabla}\widetilde{w})^2}}, \qquad \mathbf{n}_P = \frac{\mathbf{e}_z\widetilde{z} + \mathbf{e}_r\widetilde{r}}{a}. \tag{23}$$

Inserting in (22) and linearizing in $\widetilde{w}$ and ε, we obtain the condition

$$\widetilde{w} + \varepsilon - r_0\partial_r\widetilde{w} = 0 \tag{24}$$

along the contact line. At linear order in the curvatures, we may replace the radius $\widetilde{r}$ of the contact line with r_0, and thus put $\widetilde{w} = w(r_0)$. Then (24) reduces to the simple algebraic equation $-w_0(r_0) + \varepsilon + 3\xi(r_0) = 0$. Inserting the explicit expressions for w_0 and ξ gives

$$-\omega_0 + \varepsilon + (3\xi_2 - \omega_2)\cos 2\varphi = 0. \tag{25}$$

Solving for ε and ξ_2 results in the same result as those obtained from the minimization of the trapping energy in (20).

V. DISCUSSION

The main results of the present paper are given by Eqs. (18) and (21). Here we discuss their most important features and compare with the results of previous work.

A. Vertical particle position

Properly imposing Young's law along a non-circular contact line is not an easy matter. Eq. (22) relates the contact angle to the essential parameters, the slope of the interface, as expressed by the gradient $\nabla\widetilde{w}$, and the vertical position $\widetilde{z}$ of the contact line on the particle. Previous authors mostly chose to cast this in a geometrical relation for the angle α of inclination of the interface, $\tan\alpha = \nabla\widetilde{w}$, in the frame attached to the particle. We found it helpful to introduce the vertical shift ε of the particle position with respect to the tangential plane.

This approach leads to a rather simple relation of the contact angle to the interface deformation, in terms of (23) and (16). The resulting linearized differential equation (24) comprises two constraints: The term varying with the azimuthal angle determines the deformation amplitude ξ_2, whereas the constant provides the vertical shift ε. The rather simple solution (20) shows that the vertical shift is determined by the mean curvature, and the deformation amplitude by the anisotropy δc.

The vertical shift is readily confirmed for the example of a particle trapped on a spherical droplet of radius R, where our result $\varepsilon = \frac{1}{2}r_0^2/R$ can be obtained from the geometrical relation for the particle position [30, 31]. On a cylindrical interface of radius R, we find a vertical shift $\varepsilon = \frac{1}{4}r_0^2/R$; this does not agree with the discussion in Ref. [32], where a much weaker shift $\propto a^4/R^3$ was obtained.

B. Laplace pressure

The work done by the Laplace pressure turns to be essential. Like previous papers we have evaluated curvature effects by taking the flat interface as reference state. Fig. 3 shows the work in terms of the integrated volume. The integral over $\mathcal{I}$ in (9) is cancelled the term $\xi\boldsymbol{\nabla}^2 w_0$ in the interface energy (10); in physical terms the sum of the cost in deformation energy and the gain in work vanishes.

Yet the second term in (9), that is, the integral over the area occupied by the particle, results in a large negative contribution $-6\pi\gamma\omega_0^2$ to the trapping energy. The physical meaning of the integrand in $P\int dA(w_0+\varepsilon)$ becomes clear by comparing to the reference state: When switching on the curvature, the particle-free interface is shifted by w_0 with respect to the flat interface; thus adding a particle results in the work $-P\int dA(-w_0)$. On the other hand the trapped particle position is shifted by ε in downward direction, corresponding to the work $-P\int dA(-\varepsilon)$.

Thus both contributions concur to a curvature-induced enhancement of the trapping energy.

C. Trapping energy

The curvature-induced correction (21) of the trapping energy is a quadratic function of the curvature parameters H and δc,

$$E = E_F - \pi\gamma r_0^4 \left(\frac{3}{16}H^2 + \frac{1}{24}\delta c^2\right). \tag{26}$$

The numerical coefficients $-\frac{3}{16}$ and $-\frac{1}{24}$ result from several positive and negative terms of comparable size in (18). Thus it is essential to carefully evaluate all quadratic contributions to (1). An increaise of either the total curvature H or the anisotropy δc lowers the energy and enhances trapping.

We compare our Eq. (26) to the results of previous work. In an earlier paper [29], one of us considered the case of a minimal surface ($H = 0$) and found, in the notation adopted here, $E - E_F = -\frac{1}{24}\pi\gamma r_0^4\delta c^2$, which agrees with the second term in (26). In Ref. [29] the Laplace pressure and the surface energy of the particle had been discarded from the beginning; the more general approach of the present work confirms that this is justified for $H = 0$.

Kralchevsky et al. [30] and Komura et al. [31] calculated the interface energy of a particle trapped on a liquid droplet of radius R and total curvature $H = 2/R$. Expanding their result in powers of a/R and truncating at second order, we obtain $\frac{3}{16}\pi\gamma r_0^4 H^2$, in agreement with our expression for the surface energies; adding moreover the work (9) done by the Laplace pressure, $-\frac{3}{8}\pi\gamma r_0^4 H^2$, we recover the trapping energy (26).

More recently, Zeng et al. [32] considered the case of a particle trapped at a cylindrical interface of radius R, where $H = \delta c = 1/R$, and found $E - E_F = \gamma r_0^4(\frac{3}{16}\pi - 0.5333)/R^2$; the first term $\sim \frac{3}{16}$ agrees with our result for the interface energy. Note that Zeng et al. do not take into account the Laplace pressure.

D. Contact line

It turns instructive to explicitly give the position of the contact line. Inserting $\widetilde{w}$ and ε in (16) we have

$$\widetilde{z} - z_0 = \frac{r_0^2 H}{2} + \frac{r_0^2\delta c}{3}\cos(2\varphi). \tag{27}$$

The right-hand side is independent of the sign of $\cos\theta$. Thus in the case of finite H, the contact line always moves toward the convex side of the interface. If the anisotropy δc exceeds the mean curvature, the contact line may move in either direction on different parts of the contact line, depending on the ratio $\delta c/H$.

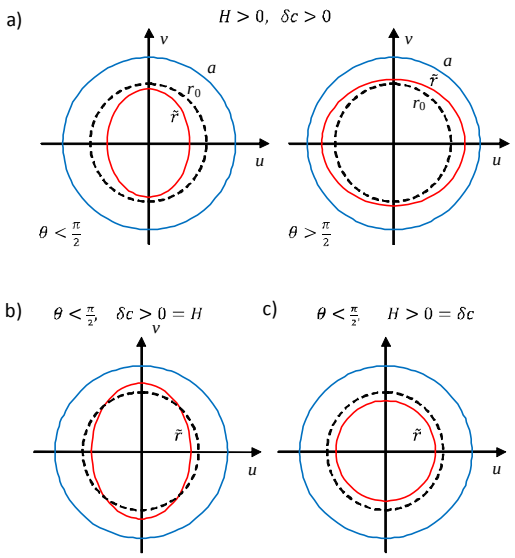

FIG. 5: Top view of the three-phase contact line on a particle of radius a. The dashed circle indicates the contact line of radius r_0 at a flat interface. The solid (red) line gives the radial coordinate $\widetilde{r}$ according to (28). a) The upper panel shows the case where both curvature parameters H and δc are positive and take similar values. For small contact angles $\theta < \frac{\pi}{2}$, the radius $\widetilde{r}$ of the contact line is reduced according to (28), whereas it increases for large contact angles $\theta > \frac{\pi}{2}$. In both cases the effect is strongest along the axis u with the largest principal curvature c_1. The lower panel illustrates the case where either H are δc vanish. b) For zero mean curvature $H = 0$, that is on a minimal surface, the radial coordinate undulates about the mean value r_0. c) In the case of zero asymmetry, $\delta c = 0$, the curvature-induced change of the radial coordinate is constant, and $\widetilde{r}$ describes a circle.

Regarding the change of the radial position, we expand (17) to linear order in $\widetilde{z} - z_0$ and find

$$\widetilde{r} - r_0 = -\frac{z_0}{r_0}\left(\frac{r_0^2 H}{2} + \frac{r_0^2\delta c}{3}\cos(2\varphi)\right). \tag{28}$$

Note that r_0 is always positive, whereas $z_0 = a\cos\theta$ takes a positive sign for small contact angles $\theta < \frac{\pi}{2}$, and a negative one for $\theta > \frac{\pi}{2}$. Thus (27) and (28) have opposite sign for small contact angles, and the same sign for large θ.

The radial modulation, that is the projection of the contact line on the $u - v$-plane, is illustrated in Fig. 5. The upper panel a) shows the case of positive H and finite δc, where the contact line moves upward and undulates around the particle; for small contact angle, the upward motion reduces the mean radius, whereas for $\theta > \frac{\pi}{2}$, it is accompanied by an increase of the radius. Fig. 5b) shows the case of zero mean curvature and finite δc, where the radius undulates along the contact line but its mean value is unchanged; a similar picture occurs for $\theta > \frac{\pi}{2}$, albeit with the axes u and v exchanged. As a last example, Fig. 5c) illustrates the case $\delta c = 0$, where the contact

line remains a cercle.

Finally we note that the above expression for the contact line relies on the quadrupolar approximation in Eq. (14), which becomes exact at large distances. Still, Eqs. (27) and (28) provide a very good description for the contact line as long as the radial change $\widetilde{r} - r_0$ can be linearized in terms of the meniscus deformation $\widetilde{z} - z_0$, in other words, as long as the derivative $d\widetilde{r}/d\widetilde{z} = -\cot\theta$ is finite. This implies that the quadrupolar approximation (14) ceases to be valid in the immediate vicinity of the poles, $\theta \approx 0$ and $\theta \approx \pi$.

E. Lateral force

On an interface with spatially varying curvature, the trapping energy changes with position and thus gives rise to a lateral force $\mathbf{F} = -\boldsymbol{\nabla} E$ on the trapped particle,

$$\mathbf{F} = \pi\gamma r_0^4 \left(\frac{3}{8} H \boldsymbol{\nabla} H + \frac{1}{12} \delta c \boldsymbol{\nabla} \delta c \right). \tag{29}$$

As shown in our previous work [29], the gradient of the curvature anisotropy pushes the particle towards more strongly curved regions of the interface. The numerical prefactor of the term proportional to $\boldsymbol{\nabla} H$ is larger by $\frac{9}{2}$.

F. Two-particle interaction

Finally we discuss curvature-induced forces between neighbor particles. Such multipole interactions are well-known for non-spherical particles [15–17]; here we consider the mutual force on spheres trapped at a curved interface. In a first step we derive the modified parameters $\widehat{H}$ and $\widehat{\delta c}$ that account for both the intrinsic curvature and additional terms due to a colloidal particle. The parameter $\widehat{H}$ is given by $\nabla^2 w = \nabla^2(w_0 + \xi)$. Since the deformation field ξ obeys the equation (12) of a minimal surface, we find $\widehat{H} = H$; in other words, the particle does not change the mean curvature of the interface.

The anisotropy is best calculated in cartesian coordinates u and v, where

$$\widehat{\delta c} = \delta c + \partial_u^2 \xi - \partial_v^2 \xi.$$

This form is readily evaluated and gives after transformation to polar coordinates

$$\widehat{\delta c} = \delta c \left(1 + \frac{r_0^4}{r^4} \cos(4\varphi) \right). \tag{30}$$

Thus the deformation field ξ significantly modifies the curvature in the vicintiy of the particle. The additonal term decays with the fourth power of the distance; because of its fourfold symmetry, the angular modulation is maximum along the principal axes u and v, and minimum in between.

Each particle feels the additional curvature induced by its neighbor. Superposition of their deformation fields gives the pair potential [29]

$$U = -\frac{\pi\gamma\delta c^2 r_0^8}{48\rho^4} \cos(4\varphi),$$

where ρ and φ describe the relative position of the particles. With the corresponding unit vectors $\mathbf{e}_\rho$ and $\mathbf{e}_\varphi$ the mutual force reads as

$$\mathbf{F}_2 = -\frac{\pi\gamma r_0^8 \delta c^2}{12\rho^5} \left(\cos(4\varphi)\mathbf{e}_\rho + \sin(4\varphi)\mathbf{e}_\varphi \right), \tag{31}$$

Thus the capillary force between two nearby particle is not a central force: Besides the attractive radial component, there is an additional force that tends to align the particles parallel to one of the principal axes. As noted previously, the latter force favors aggregates of cubic symmetry [29].

A simple estimate shows that either of the forces F_2 and F may dominate. The curvature parameters vary on the scale of the curvature radius R, resulting in curvature-induced force $F \sim \gamma r_0^4 R^{-3}$, whereas that due to pair interactions decays on the scale of the particle distance, $F_2 \sim \gamma r_0^8 \rho^{-5} R^{-2}$. With typical values $r_0 \sim 1$ μm and $R \sim 1$ mm, one finds that the ratio $F_2/F \sim R r_0^4 \rho^{-5}$ is larger than unity at distances of a few r_0, and smaller than unity beyond.

G. Comparison to gravity-curvature coupling

So far we have discarded gravity effects. We conclude by comparing the purely geometrical force (29) with the well-known force arising for heavy particles on a curved interface [8, 9, 22, 23]. The competition of weight and buoyancy results in an effective mass $m_{\text{eff}} = \frac{4}{3}\pi a^3 \varrho_{\text{eff}}$, where

$$\begin{aligned} \varrho_{\text{eff}} = (\varrho_P - \varrho_u) \left(\frac{1}{2} - \frac{3c_0}{4} + \frac{c_0^3}{4} \right) \\ + (\varrho_P - \varrho_l) \left(\frac{1}{2} + \frac{3c_0}{4} - \frac{c_0^3}{4} \right) \end{aligned} \tag{32}$$

depends on the contact angle, $c_0 = \cos\theta$, and on the densities of the particle ϱ_P, and the upper and lower fluids, ϱ_u and ϱ_l [8]. ϱ_{eff} may take either sign, depending on the contact angle and on the density contrast of the three phases. The meniscus around the particle is described by the deformation field $\zeta(r) = -(m_{\text{eff}} g/2\pi\gamma) K_0(r/\ell)$, where K_0 is a Bessel function and $\ell = \sqrt{\gamma/g\Delta\varrho}$ the capillary length. Its coupling to the intrinsic curvature,

$$E_G = \gamma \int dA \nabla\zeta \cdot \nabla w_0, \tag{33}$$

is readily integrated, $E_G = m_{\text{eff}} g H \ell^2$. A curvature gradient leads to a lateral force that has been derived by

several authors [8, 9, 22, 23]; in our notation it reads

$$F_G = -\gamma\pi a^3 \frac{4}{3}\frac{\varrho_{\rm eff}}{\Delta\varrho}\nabla H. \qquad (34)$$

where $\Delta\varrho$ is the density contrast of the fluids.

Comparison with Eq. (29) reveals that its first term $\sim \gamma\pi a^4 H\nabla H$ is by a factor aH smaller than the weight-induced force F_G. This means that the geometrical force studied here is relevant if (i) the first term $H\nabla H$ is significantly smaller than $\delta c\nabla\delta c$, or if (ii) the gravity-induced forces are small, that is, if the effective density $\varrho_{\rm eff}$ is small as compared to the density contrast $\Delta\varrho$ of the two fluids.

VI. SUMMARY

Starting from the well-known form (1), we have evaluated the trapping energy of a spherical particle to quadratic order in the curvature parameters.

(i) On a formal level, the introduction of the shift ε of the vertical partical position, leads to a remarkably simple equation (24) for Young's law at the three-phase boundary, which is solved in (20). This could be useful for disentangling the involved boundary condtions occurring at the surface of cylinders and ellipsoids [33], or on Janus particles [34].

(ii) An important contribution to the trapping energy results from the work done by the Laplace pressure on the area occupied by the particle, that is, from the second integral in (9).

(iii) As a main result, Eq. (26) shows that both the total curvature H and the anisotropy δc lower the energy and thus enhance trapping. As a consequence, both terms of the curvature-induced lateral force (29) drive particles toward strongly curved regions.

(iv) Eqs. (27) and (28) give the radial and vertical coordinates of the undulating contact line in terms of contact angle and curvature parameters; the main dependencies are illustrated in Fig. 5.

(v) The particle-induced interface deformation ξ is proportional to the curvature anisotropy δc but independent of H. As a consequence, only the anisotropy gives rise to a capillary interactions of nearby particles, and the interaction potential U reduces to the form derived previously for $\delta c \neq 0 = H$.

[1] P. Pieranski, Phys. Rev. Lett., **45**, 569 (1980).
[2] N. Bowden, A. Terfort, J. Carbeck, G.M. Whitesides, Science **11**, 233 (1997)
[3] M. Cavallaro, L. Botto, E.P. Lewandowski, M. Wang, K.J. Stebe, PNAS **108**, 20923 (2011)
[4] E. Koos, N. Willenbacher, Science **311**, 897 (2011)
[5] H.-J. Butt, Science **311**, 868 (2011)
[6] R. Aveyard, B.P. Binks, J. H. Clint, Adv. Colloid Interface Sci. **100–102**, 503 (2003)
[7] C. Zeng, H. Bissig, A.D. Dinsmore, Solid State Comm. **139**, 547, (2006)
[8] D.Y.C. Chan, J.D. Henry, L.R. White, J. Colloid Interf. Sci. **79**, 410 (1981)
[9] P.A. Kralchevsky, K. Nagayama, Langmuir **10**, 23 (1994)
[10] L. Foret, A. Würger, Phys. Rev. Lett. **92**, 058302 (2004)
[11] M. Oettel, A. Dominguez, S. Dietrich, Phys. Rev E **71**, 051401 (2005)
[12] A. Würger, L. Foret, J. Phys. Chem. B **109**, 16435 (2005)
[13] M. Oettel, A. Dominguez, S. Dietrich, J. Phys. Condens. Matter **17**, L337 (2005)
[14] K.D. Danov, P.A. Kralchevsky, J. Colloid Interf. Sci. **345**, 505 (2010)
[15] D. Stamou, D. Duschl, D. Johannsmann, Phys. Rev. E **62,** 5263 (2000)
[16] K.D. Danov, P.A. Kralchevsky, B.N. Naydenov, G. Brenn J. Colloid Interf. Sci. **287**, 121 (2005)
[17] J.-B. Fournier, P. Galatola, Phys. Rev. E **65**, 031601 (2002)
[18] E.A. van Nierop, M.A. Stejnman, S. Hilgenfeldt, Euorphys. Lett. **72**, 671 (2005)
[19] J.C. Loudet, A.M. Alsayed, J. Zhang, A. G. Yodh, Phys. Rev. Lett. **94**, 018301 (2005)
[20] B. Madivala, J. Fransaer, J. Vermant, Langmuir **25**, 2718 (2009)
[21] E.P. Lewandowski, et al., Langmuir **26**, 15142 (2010)
[22] P.A. Kralchevsky, V.N. Paunov, N.D. Denkov, K. Nagayama, J. Colloid Interf. Sci. **167**, 47 (1994)
[23] N.D. Vassileva, D. van den Ende, F. Mugele, J. Mellema, Langmuir **21**, 11190 (2005)
[24] A. Dominguez, M. Oettel, S. Dietrich, J. Chem. Phys. **128**, 114904 (2008)
[25] D.L. Hu, J.W.M. Bush, Nature **437**, 733 (2005)
[26] J.W.M. Bush, D.L. Hu, Ann. Rev. Fluid Mech. **38**, 339 (2006)
[27] P.J. Yunker, T. Still, M.A. Lohr, A.G. Yodh, Nature **476**, 308 (2011)
[28] J. Vermant, Nature **476**, 286 (2011)
[29] A. Würger, Phys. Rev. E **74**, 041402 (2006)
[30] P.A. Kralchevsky, I.B. Ivanov, K.P. Ananthapadmanabhan, A. Lips, Langmuir **21**, 50 (2005)
[31] S. Komura, Y. Hirose, Y. Nonomura, J. Chem. Phys. **124**, 241104 (2006)
[32] C. Zeng, F. Brau, B. Davidovitcha, A.D. Dinsmore, Soft Matter **8**, 8582 (2012)
[33] L. Botto, L. Yao, R.L. Leheny, K.J. Stebe, Soft Matter **8**, 4971 (2012)
[34] B.J. Park, D. Lee, ACS Nano **6**, 782 (2012)